Author Manuscript

Author Manuscript

Author Manuscript

Author Manuscript

HHS Public Access

Author manuscript

Nat Neurosci. Author manuscript; available in PMC 2015 February 01.

Published in final edited form as:

Nat Neurosci. 2014 August ; 17(8): 1055–1063. doi:10.1038/nn.3744.

Nuclear BK Channels Regulate Gene Expression via the Control of Nuclear Calcium Signaling

Boxing Li[1,2], **Wei Jie**[1,2], **Lianyan Huang**[3], **Peng Wei**[1,2], **Shuji Li**[1,2], **Zhengyi Luo**[1,2], **Allyson K. Friedman**[4], **Andrea L. Meredith**[5], **Ming-Hu Han**[4], **Xin-Hong Zhu**[1,2], and **Tian-Ming Gao**[1,2,*]

[1]State Key Laboratory of Organ Failure Research, Department of Neurobiology, School of Basic Medical Sciences, Southern Medical University, Guangzhou 510515, China

[2]Key Laboratory of Neuroplasticity of Guangdong Higher Education Institutes, Southern Medical University, Guangzhou 510515, China

[3]School of Public Health and Tropical Medicine, Southern Medical University, Guangzhou 510515, China

[4]Department of Pharmacology and Systems Therapeutics, Friedman Brain Institute, Icahn School of Medicine at Mount Sinai, New York, New York 10029, USA

[5]Department of Physiology, University of Maryland School of Medicine, Baltimore, MD 21201, USA

Abstract

Ion channels are essential for the regulation of neuronal functions. The significance of plasma membrane, mitochondrial, endoplasmic reticulum, and lysosomal ion channels in the regulation of Ca^{2+} is well established. In contrast, surprisingly less is known about the function of ion channels on the nuclear envelope (NE). Here we demonstrate the presence of functional large-conductance, calcium-activated potassium channels (BK channels) on the NE of rodent hippocampal neurons. Functionally blockade of nuclear BK channels (nBK channels) induces NE-derived Ca^{2+} release, nucleoplasmic Ca^{2+} elevation, and cAMP response element binding protein (CREB)-dependent transcription. More importantly, blockade of nBK channels regulates nuclear Ca^{2+}-sensitive gene expression and promotes dendritic arborization in a nuclear Ca^{2+}-dependent manner. These results suggest that nBK channel functions as a molecular linker between neuronal activity and nuclear Ca^{2+} to convey the signals from synapse to nucleus and is a new modulator for synaptic activity-dependent neuronal functions at the NE level.

Users may view, print, copy, and download text and data-mine the content in such documents, for the purposes of academic research, subject always to the full Conditions of use:http://www.nature.com/authors/editorial_policies/license.html#terms

*Corresponding Author: Dr. Tian-Ming Gao Department of Neurobiology, School of Basic Medical Sciences Southern Medical University 1088 Guangzhou Ave North, Guangzhou, 510515, China Telephone: +86-20-6164-8617 Fax: +86-20-6164-8161 tgao@smu.edu.cn.

The authors declare no competing financial interests.

Author contributions:

B.L. and TM.G. designed the study; B.L., W.J., L.H. conducted biochemistry, Ca imaging, immunocytochemistry experiments; B.L., P.W., and Z.L. conducted electrophysiological experiments, B.L. and S.L., cultured neurons; A.K.F, A.L.M, MH.H, and XH. Z. contributed new reagents/analytic tools; B.L., W.J., P.W., Z.L., and L.H. collected and analyzed data; B.L., L.H., and TM.G. wrote the manuscript.

A supplementary methods checklist is available

Author Manuscript Author Manuscript Author Manuscript Author Manuscript

Keywords

nuclear ion channel; excitation-transcription coupling; nuclear Ca^{2+} signaling; BK channel

As transmembrane proteins, ion channels are present not only on the plasma membrane but also on intracellular membrane-bound organelles. Much is known regarding plasma membrane ion channels controlling action potential firing, synaptic transmission, and gene expression through the regulation of membrane potential and Ca^{2+} influx[1]. In addition, the significance of mitochondrial[2], lysosomal[3,4], and endoplasmic reticulum (ER)[5] ion channels in regulating ATP production, stress response and apoptosis via the control of Ca^{2+} signals has been well established. In contrast, despite the obvious structural and functional importance of the nucleus in gene expression and regulation, the functions of ion channels on the NE (nuclear ion channels) remain largely unknown, especially in neurons.

Recent studies have shown that the NE is a key source of nucleoplasmic Ca^{2+}: Ca^{2+} in perinuclear space, the lumen between the outer and the inner nuclear membrane of NE, can be released into the nucleoplasm via nuclear inositol 1,4,5-trisphosphate receptors (IP_3R) and ryanodine receptors (RyR)[6–10]. Therefore, the NE is a functional perinuclear Ca^{2+} store and is independent from the ER and cytoplasm in regulating the nucleoplasmic Ca^{2+} concentration ($[Ca^{2+}]_{nu}$)[6–10]. Meanwhile, numerous studies have demonstrated that nucleoplasmic Ca^{2+} is one of the most important signals in mediating neuronal activity-dependent gene expression[11,12], and is critical for several long lasting adaptive responses, including modulation of synapse formation and dendritic complexity[13], regulation of synaptic plasticity and memory consolidation[13,14], and activity-dependent acquired neuroprotection[12,15].

As a key signal in neuronal functions, numerous fundamental questions remain such as how this NE-derived Ca^{2+} release regulated in neurons, whether it can be regulated by nuclear ion channels through changing the NE transmembrane potential, similar to the regulation of Ca^{2+} fluxes in the plasma membrane and mitochondria, which type of nuclear ion channel governs this transmembrane potential change, and whether this nuclear ion channel also regulate transcription factor activation and gene expression induced by neuronal activity. To address these questions, we applied a combination of biochemical and molecular biological methods, together with calcium imaging, voltage imaging, and patch clamp techniques in wild-type and gene knockout mice to study the function of the nuclear ion channel. We found that functional BK channels are present on the NE of hippocampal neurons. Pharmacological or genetic blockade of nBK channels directly regulates the NE-derived release of Ca^{2+}, CREB phosphorylation, gene expression, and dendritic arborization, suggesting that nBK channels play a key role in neuronal activity-dependent functions and serve as new molecular link between neuronal activities, nuclear Ca^{2+} signaling, and gene expression at the NE level.

Author Manuscript Author Manuscript Author Manuscript Author Manuscript

RESULTS

BK channels are expressed on the NE

To investigate the subcellular localization of BK channels in intact hippocampal neurons, we used a monoclonal antibody for the α subunit of the BK channel in immunocytochemistry[16]. The confocal optical sections demonstrated an intracellular ring-like labeling around the nucleus (**Fig. 1a**). Analysis of intensity profiles indicated that the labeling was co-localized with the NE marker lamin B, suggesting that the BK channels are localized to the NE (**Fig. 1a**). To confirm that this observation did not result from non-specific binding of the BK antibody, we conducted the same experiment in the neurons from BK channel α subunit-null mice (*Kcnma1*$^{-/-}$) mice. As shown in **Fig. 1a**, the BK channel antibody failed to detect any signal in the neurons from *Kcnma1*$^{-/-}$ mice, validating its specificity. Furthermore, we used immunoelectron microscopy to investigate BK channel localization at high spatial resolution. As shown in **Fig. 1b**, gold particles signaling BK channels were localized on the NE (**Fig. 1b**), further confirming the NE localization of the BK channels. Consistent with previous findings[17,18], we also observed the mitochondrial localization of the BK channels (**Fig. 1b**). The negative labeling in *Kcnma1*$^{-/-}$ mice once again validated the specificity of the BK antibody (**Fig. 1b**). To further verify the nuclear localization of the BK channels, we isolated nuclei from cultured hippocampal neurons. A ring-like labeling of BK channel immunofluorescence was detected in the isolated nuclei from wild-type mice (**Fig. 1c**). Analysis of intensity profiles of the isolated nuclei indicated that BK channel were co-localized with lamin B (**Fig. 1c**). The BK channel antibody failed to detect any signal in the nucleus from *Kcnma1*$^{-/-}$ mice (**Fig. 1c**). Additionally, we transfected neurons with a green fluorescent protein (GFP)-tagged BK channel construct. As shown in **Fig. 1d**, green fluorescence was detected around the nucleus and co-localized with lamin B, once again suggesting the NE localization of the BK channels. This interpretation was further supported by subcellular fractionation and immunoblot analysis: BK channels were detected on the nuclear fraction, as well as the plasma membrane fraction and the whole cell lysate (**Fig. 1e**). The purity of the nuclear fraction was validated by the presence of lamin B, and the absence of cytosolic marker GAPDH, ER marker calnexin and mitochondrial marker COX IV (**Fig. 1e**). The presence of immunoreactivity in the NE fraction, but not in the denuded nuclei (NE-depleted nuclei) fraction further verified the localization of the BK channel on NE (**Fig. 1f**). The absence of the immunobands in *Kcnma1*$^{-/-}$ mice confirmed that the immunoreactivity arose from authentic BK channels (**Fig. 1e,f**).

Besides the pore-forming α subunit, BK channels also contain auxiliary β subunits. The brain-specific auxiliary subunits β4 were also observed and co-localized with lamin B (**Supplementary Fig. 1**), suggesting that a fully assembled BK channel complex is localized on NE. To further determine whether the nuclear BK channels (nBK channels) are functional and exhibit similar electrophysiological properties to the plasma membrane BK channels (pmBK channel), we performed single channel recordings with patch clamp on isolated nuclei. We recorded a voltage-dependent and Ca^{2+} -dependent K^+ channel activity with a conductance of approximately 220 ps, similar to that of neuronal pmBK channel[19–22] (**Fig. 1g–i**). The blockade of the channel activity with paxilline, a BK channel-specific blocker, and the absence of the channel activity in *Kcnma1*$^{-/-}$ mice further confirmed that

Author Manuscript Author Manuscript Author Manuscript Author Manuscript

the channel activity arose from BK channels (**Fig. 1g,h**). Taken together, these observations demonstrate that BK channels are present and functional on the NE of hippocampal neurons.

nBK channels regulate nuclear Ca^{2+} concentrations

pmBK channels exhibit significant abilities in controlling the plasma membrane potential and accordingly regulating the voltage-dependent calcium influx[19–22]. nBK channels, with similar electrophysiological properties to pmBK channels, may also regulate the nuclear transmembrane potential ($\Delta\Psi_n$), thereby regulating nuclear calcium concentration. To address this hypothesis, we first examined whether nBK channels could regulate the $\Delta\Psi_n$. Isolated nuclei were loaded with $DiOC_6(3)$, which has been validated as a potentiometric probe in NE[23,24]. Paxilline elicited a consistent increase in $DiOC_6(3)$ fluorescence (0.28 ± 0.02 $\Delta F/F_0$ (mean ± s.e.m.), $n = 20$), indicating that the perinuclear lumen became more negative[23,24] (**Fig. 2a**). Consistently, the paxilline-induced $\Delta\Psi_n$ was completely absent in the nuclei from *Kcnma1*$^{-/-}$ mice (0.02 ± 0.01 $\Delta F/F_0$ (mean ± s.e.m.), $n = 31$, unpaired *t*-test, $P = 2.81 \times 10^{-13}$, $t_{49} = 9.90$, compared with wild-type group) (**Fig. 2a**). These results suggest that nBK channels can regulate $\Delta\Psi_n$.

Next, we investigated whether nBK channels can regulate $[Ca^{2+}]_{nu}$ in hippocampal neurons. Paxilline is membrane permeable and inhibits BK channels on both the plasma membrane and intracellular organelles. IbTx, a membrane-impermeant BK channel blocker, only inhibits pmBK channels on the plasma membrane. Calcium imaging of the confocal mid-nuclear section (**Fig. 2b**) demonstrated that paxilline induced $[Ca^{2+}]_{nu}$ elevation in intact neurons, whereas IbTx lacked an influence on $[Ca^{2+}]_{nu}$ (**Fig. 2c**). Moreover, paxilline elicited $[Ca^{2+}]_{nu}$ elevation even after complete blockade of the pmBK channels with a high concentration of IbTx (100 μM)[20] (**Fig. 2c**), which suggests that the effect of paxilline was mainly mediated by intracellular BK channels, but not pmBK channels. This idea was further supported by the results that paxilline induced $[Ca^{2+}]_{nu}$ elevation in digitonin-permeabilized neurons with a Ca^{2+}-buffered intracellular medium (**Fig. 2d**). Paxilline-induced $[Ca^{2+}]_{nu}$ elevation was largely suppressed by prior depletion of intracellular Ca^{2+} store with thapsigargin, but not by EGTA-buffered extracellular Ca^{2+} (**Fig. 2c**), further suggesting that the nucleoplasmic Ca^{2+} transient is likely due to direct Ca^{2+} release from NE[8, 24]. Importantly, neurons from *Kcnma1*$^{-/-}$ mice were completely devoid of paxilline-induced $[Ca^{2+}]_{nu}$ elevation (**Fig. 2e**). Taken together, these results strongly supported the idea that the intracellular BK channels and perinuclear Ca^{2+} store are responsible for eliciting nuclear Ca^{2+} signals.

To further verify that the mediators of the paxilline-induced $[Ca^{2+}]_{nu}$ elevation are the nBK channels and perinuclear Ca^{2+} store, isolated nuclei from cultured hippocampal neurons were loaded with either the Ca^{2+} probe Fluo-4/AM or Fluo-4/dextran. Fluo-4/AM, a membrane-permeant probe, preferentially accumulated in the NE (**Fig. 2f**), whereas Fluo-4/dextran, a membrane-impermeant probe, was distributed uniformly in the nucleoplasm[8,10,24](**Fig. 2g**). Confocal microscopy revealed that paxilline produced opposite Ca^{2+} changes in the NE and the nucleoplasm. Application of paxilline led to a decrease of NE Ca^{2+} (**Fig. 2f**), which paralleled a transient Ca^{2+} increase in the nucleoplasm (**Fig. 2g**). The paxilline-induced Ca^{2+} transient was largely diminished by knockdown of BK channel

Author Manuscript Author Manuscript Author Manuscript Author Manuscript

with lentiviral shRNAs (**Supplementary Fig. 2**), and was completely abolished in neurons from *Kcnma1*$^{-/-}$ mice (**Fig. 2f,g,** Fluo-4/AM intensity, 0.29 ± 0.03 $\Delta F/F_0$ in wild-type group, 0.01 ± 0.02 $\Delta F/F_0$ for *Kcnma1*$^{-/-}$ group, n = 25 for each group, unpaired t-test, $P = 1.16 \times 10^{-10}$, $t_{48} = 8.19$; Fluo-4/dextran intensity, 0.33 ± 0.04 $\Delta F/F_0$ in wild-type group, 0.03 ± 0.02 $\Delta F/F_0$ for *Kcnma1*$^{-/-}$ group, n = 22 for each group, unpaired t-test, $P = 2.12 \times 10^{-8}$, $t_{42} = 6.89$, data is presented as mean ± s.e.m.). Depletion of the perinuclear Ca^{2+} store with thapsigargin completely blocked paxilline-induced Ca^{2+} transient (**Fig. 2h**), suggesting that the perinuclear Ca^{2+} store are responsible for eliciting the paxilline-induced nuclear Ca^{2+} signals.

Numerous studies have demonstrated that IP_3R and RyR, located on the inner membrane of the NE, mediate the release of Ca^{2+} from the perinuclear space into the nucleoplasm[6,10]. Therefore, we used specific IP_3R inhibitors (heparin and 2-APB) and a RyR inhibitor (ruthenium red) to test which receptor is responsible for the nBK channel-regulated NE Ca^{2+} release. The paxilline-induced Ca^{2+} release was attenuated by 10 μM ruthenium red and was completely blocked by 100 μM ruthenium red (**Fig. 2h**). Conversely, results with the IP_3R blockers indicated that neither heparin (50 μM) nor 2-APB (100 μM) affected paxilline-induced Ca^{2+} release (**Fig. 2h**). To further confirm that RyRs mediate paxilline-induced Ca^{2+} release, we designed two independent shRNAs to knock down RyRs expression in neurons[25]. RyRs expression level was reduced to 56.4% and 51.5% of control by using the shRNA individually, and was reduced to 25.5% when both shRNAs were used together (**Supplementary Fig. 3**). As shown in **Fig. 2i**, knockdown of RyRs significantly compromised paxilline-induced $[Ca^{2+}]_{nu}$ elevation in intact neurons, providing direct evidence that RyRs mediate the paxilline-induced Ca^{2+} release. Collectively, these results indicate that blockade of nBK channel induces NE-derived Ca^{2+} release and $[Ca^{2+}]_{nu}$ elevation via RyRs.

nBK channels regulate nuclear Ca^{2+} signaling

Activity-dependent activation of CREB is heavily implicated in neuronal development and plasticity, long-term memory formation, and cell survival[12,15,26,27]. Elevation of $[Ca^{2+}]_{nu}$ results in the phosphorylation of CREB on its activator site serine 133, which is often regarded as a marker for CREB-mediated transcription[28,29]. Because blockade of the nBK channels induced $[Ca^{2+}]_{nu}$ elevation, we therefore further investigated whether the nBK channels could also induce CREB phosphorylation in isolated nuclei and intact neurons.

Using immunoblot in isolated functional nuclei, we observed that paxilline induced the phosphorylation of CREB, similar to the response to elevate free Ca^{2+} (**Fig. 3a**). The same results were also observed in immunofluorescence experiments (**Fig. 3b,c**). The role of the nBK channels in regulating CREB phosphorylation was further verified in isolated nuclei from wild-type and *Kcnma1*$^{-/-}$ mice. As shown in **Fig. 3d**, paxilline induced CREB phosphorylation only in nuclei from wild-type mice, but not in nuclei from *Kcnma1*$^{-/-}$ mice.

CREB is a target for two Ca^{2+}-regulated signaling pathways, the Ca^{2+}/calmodulin (CaM)-dependent protein kinases, in particular the nuclear CaM kinase IV (CaMKIV)[28,29], and the MAP kinase/extracellular signal-regulated kinase (ERK) cascade[30]. As shown in **Fig. 3a** and

Author Manuscript Author Manuscript Author Manuscript Author Manuscript

d, the nuclear CaMKIV were activated (phosphorylation in Thr196) by paxilline, as well as by the increase of the free Ca^{2+} concentration, suggesting the involvement of CaMKIV in paxilline-induced CREB phosphorylation (**Fig. 3a**). In contrast, due to the lack of cytoplasmic and plasma membrane-associated proteins in isolated nuclei, ERK1/2 were not activated by paxilline (**Fig. 3a,d**). In addition, paxilline-induced CREB phosphorylation in isolated nuclei was blocked by the selective CaMKIV pathway (CaM kinase kinase (CaMKK)) inhibitor STO-609, but not by the ERK pathway inhibitor U0126 (**Fig. 3e**). These results indicate that paxilline-induced CREB phosphorylation is likely catalyzed by nuclear CaM kinases, but not ERK, which is consistent with studies showing that CaMKIV mediates $[Ca^{2+}]_{nu}$ elevation-induced CREB phosphorylation[31].

To further confirm the roles of nuclear Ca^{2+} and CaMKIV, we conducted similar experiments in intact hippocampal neurons. Similar to the results in isolated nuclei, paxilline induced CREB phosphorylation even after pmBK channel blockade by IbTx pretreatment (**Fig. 3f** and **Supplementary Fig. 4**). This event was counteracted by STO-609, but not by U0126 (**Fig. 3g**). Additionally, to provide the direct evidence for the role of CaMKIV, we used shRNAs to knock down the CaMKIV expression (**Fig. 3h**). As shown in **Fig. 3i**, CaMKIV-specific shRNAs significantly inhibited paxilline-induced CREB phosphorylation, further confirming the critical role of CaMKIV in paxilline-induced pCREB. Furthermore, we specifically blocked nuclear Ca^{2+} signaling by overexpressing the nuclear-targeted Ca^{2+} buffering protein parvalbumin (PV-NLS)[32] and kinase-inactive form of CaMKIV (CaMKIVK75E), which functions as a dominant negative mutant of CaMKIV (dnCaMKIV)[12,13]. As shown in **Fig. 3j**, the induction of CREB phosphorylation by paxilline was reduced in hippocampal neurons transfected with PV-NLS or dnCaMKIV, but not in U0126-treated neurons. Collectively, these results indicate that blockade of nBK channels induces CREB phosphorylation in a nuclear Ca^{2+}/CaMKIV-dependent manner.

nBK channels regulate activity-evoked gene expression

Synaptic excitation on the dendritic spines of pyramidal neurons induces transcription factor activation and gene expression in the nucleus. This excitation-transcription (E-T) coupling is critically important for a broad range of processes and behaviors, including neuronal development, learning and memory, and cell survival[12,29,31]. To identify the role of nBK channels in E-T coupling, we investigate the effects of the nBK channels on the regulation of synaptic activity-evoked CREB phosphorylation and gene expression.

Hippocampal neurons were preincubated with IbTx to exclude the involvement of pmBK channels (**Supplementary Fig. 4**) and were stimulated with the $GABA_A$ receptor antagonist, bicuculline (50 μM). GABAergic interneurons exert a tonic inhibition onto the network. Removal of GABAergic inhibition with bicuculline leads to enhancement of neuronal activity and induces robust $[Ca^{2+}]_{nu}$ elevation and CREB phosphorylation[12,31] (**Fig. 4a**). Bicuculline-induced $[Ca^{2+}]_{nu}$ elevation and CREB phosphorylation are highly dependent on the filling of the perinuclear Ca^{2+} store, and a reduction of the Ca^{2+} store will significantly compromise the bicuculline-induced effects[31]. As shown in **Fig. 4a,b**, paxilline pretreatment attenuated both bicuculline-induced $[Ca^{2+}]_{nu}$ elevation and CREB phosphorylation in wild-type mice because paxilline induced the reduction of the perinuclear

Author Manuscript Author Manuscript Author Manuscript Author Manuscript

Ca^{2+} store content in advance (**Fig. 4a,b** and **Fig. 2**). In contrast, paxilline failed to compromise bicuculline-induced $[Ca^{2+}]_{nu}$ elevation and CREB phosphorylation in the neurons from *Kcnma1*$^{-/-}$ mice (**Fig. 4a,b**).

To determine whether the effects of nBK channels blockade extended to differences in activity-evoked gene transcription, we performed Real Time quantitative Reverse Transcription PCR (qRT-PCR) to analyze the expression of activity-dependent and nuclear Ca^{2+}-sensitive genes[12,33,34] after IbTx preincubation. Indeed, paxilline induced increases in *c-fos*, *Npas4*, *Atf3*, *Btg2*, *Bcl6* and *Ifi202b* expression (**Fig. 4c–h**), but not *GADD45β* and *GADD45γ* expression (data not shown), during basal neuronal activity. Paxilline-induced genes expression was blocked by STO-609 and was completely abolished in the neurons from *Kcnma1*$^{-/-}$ mice (**Fig. 4c–h**). Similar to the effects on bicuculline-induced $[Ca^{2+}]_{nu}$ and CREB phosphorylation, paxilline pretreatment significantly attenuated bicuculline-induced elevation of the genes expression (**Fig. 4c–h**). Taken together, these results indicate that the nBK channels play an important role in regulating synaptic activity-evoked CREB phosphorylation and gene expression in E-T coupling.

nBK channels regulate dendritic arborization

Dendritic arborization is critically important for neuronal development and function, and the regulation of dendritic geometry is highly dependent on E-T coupling[13]. Given that the nBK channel is important in controlling nuclear Ca^{2+} signaling (**Fig. 2 and 3**) and gene expression (**Fig. 4**) in E-T coupling, we further explored the roles of nuclear Ca^{2+} signaling and the nBK channels in the regulation of dendritic arborization.

To first determine the role of nuclear Ca^{2+} signaling in the regulation of dendritic arborization in basal condition, we expressed CaMBP4 or dnCaMKIV in hippocampal neurons. CaMBP4 contains four repeats of the M13 CaM binding peptide and can effectively inactivate the nuclear Ca^{2+}/CaM complex and block genomic responses induced by nuclear Ca^{2+} signaling[12,13,15]. Consistent with the previous study[13], morphological analyses showed that the expression of CaMBP4 or dnCaMKIV could reduce the dendritic complexity assessed by Sholl analysis and the dendritic length (**Fig. 5a,b**), suggesting that nuclear Ca^{2+} signaling is important for the basal dendritic arborization.

To further investigate the role of nBK channels in the regulation of dendritic arborization, hippocampal neurons were pretreated with IbTx to exclude the involvement of pmBK channel (**Fig. 5** and **Supplementary Fig. 4**). Morphometric analyses revealed that neurons treated with paxilline showed a significant increase both in the complexity of the dendrites (**Fig. 5a**) and in the total dendritic length (**Fig. 5b**). Importantly, this paxilline-induced increase was reversed by the expression of CaMBP4 or dnCaMKIV (**Fig. 5a,b**), suggesting that paxilline-induced increase in dendritic complexity and length is also dependent on the nuclear Ca^{2+} signaling. Similarly, neurons transfected with BK channel-specific shRNAs showed a significant increase both in the dendritic complexity and in the total dendritic length (**Fig. 5c,d**). STO-609 suppressed basal dendritic arborization and reversed the shRNA-induced increase, once again suggesting that both basal and paxilline-induced dendritic arborizations are dependent on nuclear Ca^{2+} signaling. To determine the specific

Author Manuscript Author Manuscript Author Manuscript Author Manuscript

genes mediating paxilline-induced morphological changes, we used shRNAs to knock down the expression of nBK channel-target genes (**Supplementary Fig. 5**). As shown in **Fig. 5e,f** and **Supplementary Fig. 6**, only shRNA against *Npas4* significantly reduced dendritic arborization, and reversed paxilline-induced morphological changes, suggesting the involvement of *Npas4* in both basal and paxilline-induced dendritic arborization. Taken together, these results indicate that nBK channels can regulate dendritic arborization in a nuclear Ca^{2+}/CaMKIV signaling-dependent manner.

DISCUSSION

In this study, we demonstrate for the first time to our knowledge that functional BK channels are expressed on the NE of hippocampal neurons and that the activities of nBK channels regulate synaptic activity-triggered nuclear Ca^{2+} signal, CREB activation, gene expression, and dendritic arborization. These findings reveal the important role of the nBK channel as a key regulator and molecular linker between neuronal activities, nuclear Ca^{2+} signaling, and gene expression at the NE level.

The positive expression of BK channels in the nuclear envelope was based on immunofluorescence, immunoelectron microscopy and immunoblot data in both intact cells and isolated nuclei (**Fig. 1a–f**). The use of *Kcnma1*$^{-/-}$ mice further confirmed the specificity of the labeling (**Fig. 1**). Most importantly, excised patches of nuclear membrane confirmed the presence of the nBK channels that exhibit similar voltage-dependence, Ca^{2+}-dependence, single channel conductance and pharmacological properties to the BK channels found in the plasma membrane (**Fig. 1g–i**). Thus, several independent lines of evidence indicate the presence of functional BK channels in the NE, supporting the notion that the BK channels have multiple sites of function, including the plasma membrane[22,35-37], mitochondria[17,18,38], and, as shown here, the NE.

Nuclear Ca^{2+} is a potent signal in regulating neuronal gene expression, and represents a key player in the dialog between synapse and nucleus[11,12,31]. However, the source of nuclear Ca^{2+} has been debated for many years[6], and the mechanisms by which nuclear Ca^{2+} is regulated by synaptic activity are incompletely understood. It has been proposed that the nuclear pore complex (NPC) is large enough to provide routes for passive diffusion of ions to cross the NE, which would imply that nuclear Ca^{2+} signaling is dependent on cytosolic Ca^{2+} changes[6,7]. However, numerous evidences suggested that nucleus has an autonomous Ca^{2+} signaling system, which can generate its own independent Ca^{2+} transients[6–10]. (1) NPC size is regulated by the filling state of the NE lumen. Depletion of perinuclear Ca^{2+} stores has been shown to induce a conformational change of the NPC and reduce the NPC permeability[6]. (2) The ability to obtain high-resistance gigaohm seals during patch clamping in the nucleus-attached mode, when dozens of NPCs may be encompassed by the patch pipette, suggested that the NPCs can exist in a closed state that restricts ion flow[39]. (3) The ion movement seems not freely across NPC, because studies show that there are differences in ion concentrations between cytoplasm and nucleoplasm[40–43]. (4) When HepG2 cells were stimulated with extracellular ATP, nucleoplasmic Ca^{2+} signal preceded cytosolic Ca^{2+} signal by ~450 ms, suggesting the independence of nucleoplasmic Ca^{2+} signal[9]. (5) In the present study, application of paxilline to intact neurons induces nucleoplasmic Ca^{2+}

Author Manuscript Author Manuscript Author Manuscript Author Manuscript

elevation without raising cytosolic Ca^{2+} concentration **(Fig. 2b)**, suggesting that the nucleoplasmic Ca^{2+} is independent from cytoplasmic Ca^{2+} and NPC-mediated Ca^{2+} transport. Nonetheless, the existence of this autonomous nuclear Ca^{2+} signaling system does not exclude the presence of the NPC-mediated Ca^{2+} transport.

Partly due to a lack of suitable experimental methods, the ionic gradient for K^+ across the NE remains unknown in intact cells. Recent studies in isolated nuclei loaded with K^+-sensitive fluorescent indicators showed that the K^+ concentration in the perinuclear space is much lower than the cytoplasm and nucleoplasm[41]. Therefore the changes in the nuclear K^+ channel activity would alter the K^+ flux across the NE and ultimately lead to the alteration of the $\Delta\Psi_n$. Indeed, our results showed that the nBK channels, with the similar electrophysiological properties to pmBK channels (**Fig. 1g–i**), regulate the $\Delta\Psi_n$ (**Fig. 2a**), supporting the existence of the K^+ gradient across the NE. Nevertheless, all these results were obtained from isolated nuclei, and need further confirmation in intact cells. It is noteworthy that the open probability of RyRs is elevated upon changes of voltage[24,44–46]. Thus, it is highly probable that RyRs may be affected by paxilline-induced $\Delta\Psi_n$ as revealed by the voltage-sensor $DiOC_6(3)$ (**Fig. 2a**). Similar voltage-induced RyRs-mediated Ca^{2+} release were observed in pancreatic beta cells[24]. Nonetheless, we do not exclude the existence of other voltage-sensitive pathways that directly or indirectly trigger the release of nuclear calcium[24].

Coupling between synaptic excitation and gene expression is critical for a broad range of long-term changes in nervous system functions. Although many intracellular molecules, such as calmodulin, MAPKs and CaMKs, have been shown to participate in synapse-to-nucleus signaling, faster modulators are also required to convey fast information-laden synaptic electrical signals[6,26]. Via rapid ion channel kinetics, the nBK channel may function as a fast molecular modulator between neuronal activity and nuclear Ca^{2+} to convey the signaling from synapse to nucleus. The NE is inaccessible to analysis with patch clamp pipettes and voltage-sensitive dyes in intact neurons, which makes it difficult to measure the activity of nBK channels synchronously during neuronal activity. Therefore, the effects of neuronal activity on the activity of the nBK channel require further exploration. It is noteworthy that neuronal activity can modulate the pmBK channels in a bi-directional manner: activity-induced intracellular Ca^{2+} elevation and CaMKII activation activate pmBK channels[47], whereas activity-induced calcineurin activation has the opposite effect[48]. If the same regulation also applies to nBK channels, the regulation of nBK channel activity by neuronal activity may be bi-directional as well. The development of suitable experimental systems will help to elucidate this question.

The long-term maintenance of activity-induced, functional adaptations requires nuclear Ca^{2+} signaling-dependent, CREB-mediated transcription to activate gene expression[12,15,26–28]. Using immunofluorescence, immunoblot and qRT-PCR, we show that blockade of the nBK channel increases CREB phosphorylation and neuronal activity-dependent gene expression during basal neuronal activity, but compromises those during bicuculline-induced action potential bursting (**Fig. 3** and **4**). Bicuculline-induced CREB phosphorylation and gene expression need sustained, Ca^{2+} store-derived nuclear Ca^{2+} elevation, and depletion of the Ca^{2+} store will significantly compromise these effects[31]. In our studies, paxilline

Author Manuscript Author Manuscript Author Manuscript Author Manuscript

pretreatment induced the release of nuclear Ca^{2+} and the reduction of the Ca^{2+} store content (**Fig. 2**), and consequently, compromise the bicuculline-induced nuclear Ca^{2+} elevation needed for CREB phosphorylation and gene expression (**Fig. 4**). These results are consistent with studies proposing that filling of the nuclear Ca^{2+} store is required for synaptically evoked nuclear Ca^{2+} signaling and CREB-mediated gene expression[31]. nBK channel-modulated CREB phosphorylation and gene expression is dependent on nuclear Ca^{2+} signaling because specific blockade of nuclear Ca^{2+} signaling via dnCaMKIV, PV-NLS, and STO-609, but not via the ERK inhibitor U0126, abolished the effects of nBK channel blockade (**Fig. 4**). In the intact cell, we cannot exclude the possibility that Ca^{2+} release from other organelles may drive gene expression in our conditions. However, as shown in **Fig. 2** and **3**, the NE would be responsible for an important part of these intracellular Ca^{2+} signals.

The dendritic tree determines the neuronal connectivity and has a strong influence on synaptic transmission and integration of synaptic signals. Moreover, dendritic geometry itself is regulated by neuronal activity. Our results show here that nBK channel blockade causes a significant increase both in the total dendritic length and in the complexity of the dendrites (**Fig. 5**), further confirming the importance of nuclear Ca^{2+} in the regulation of dendritic arborization[13]. Knockdown of one of the nBK channel-target gene, *Npas4*, expression completely blocked paxilline-induced morphological changes, indicating the critical role of Npas4 in this regulation. Importantly, Npas4 also functions as a transcriptional regulator, with a key role in activity-dependent regulation of inhibitory synapse development[33], contextual memory formation[34], and neuronal protection[12,49]. Knockdown of Npas4 significantly inhibits brain-derived neurotrophic factor (BDNF) expression[11,33], implicating the potential mechanisms by which Npas4 knockdown blocks paxilline-induced morphological changes.

By controlling nuclear Ca^{2+} signaling, the nBK channel links neuronal activity to the regulation of CREB activation and gene expression, the control of total dendritic length and branching patterns. The blockade of the nBK channels represents a new strategy for the development of effective therapies for the reduction of dendrite complexity in aging, Alzheimer's disease and autism[11,33]. These findings may also help explain the various phenotypes, such as Purkinje cell dysfunction[37], cerebellar ataxia[35,37], and abnormal circadian behavioral rhythms[36], found in BK channel global knockout mice.

METHODS Reagents and antibodies

Paxilline, IbTx, STO-609, thapsigargin, EGTA, ruthenium red, heparin, digitonin, 2-APB, U0126, bicuculline, DMSO, DAPI and all the other reagents to make solutions were from Sigma-Aldrich. Fluo-4/AM, Fluo-4/dextran, X-Rhod-1 were from Life Technologies. Antibodies specific for BK channel α-subunit (L6/60, Millipore MABN70, immunocytochemisty (ICC) 20 μg/ml, western blot (WB) 10 μg/ml, reference (Ref.) PMID 16566008), BK channel β4-subunit (Alomone Lab APC-061, ICC 1:100, Ref. PMID 21697543), Lamin B (Abcam ab16048, WB 1:1000, ICC 1:500, Ref. PMID 24265311) GAPDH (Cell Signalling 3683S, WB 1:1000, Ref. PMID 22895339), Calnexin (Cell Signalling 2433S, WB 1:1000, Ref. PMID 19815548), COX IV (Cell Signalling 4850S, WB 1:1000, Ref. PMID 19737931), phospho-CREB (Cell Signalling 9198S, WB 1:1000, ICC

Author Manuscript Author Manuscript Author Manuscript Author Manuscript

1:500, Ref. PMID 17906627), CREB (Cell Signalling 9197S, WB 1:1000, Ref. PMID 20864036), phospho-CaMKIV (Santa Cruz Biotechnology sc-28443-R, WB 1:200, Ref. PMID 18559891), CaMKIV (Cell Signalling 4032S, WB 1:1000, Ref. PMID 21784978), phospho-ERK (Cell Signalling 9101S, WB 1:1000, Ref. PMID 11782377), and ERK (Cell Signalling 9102S, WB 1:1000, Ref. PMID 21669876), actin (Cell Signalling 4967S, WB 1:1000, Ref. PMID 17525163), RyR (Thermo MA3-925, WB 1:1000, Ref. PMID 1645737), Na/K ATPase (Cell Signalling 3010S, WB 1:1000, Ref. PMID 21724843) were used.

Cell culture and transfection and virus infection

Wild-type or *Kcnma1*$^{-/-}$ mice (C57BL/6J strain) and Sprague-Dawley rats were used for cell culture. All of the experiments were conducted in accordance with the Regulations for the Administration of Affairs Concerning Experimental Animals (China) and were approved by the Southern Medical University Animal Ethics Committee. Three to four animals were housed per cage on a 12 h light, 12 h dark cycle, similar to those reported in previous publications. Pure primary hippocampal neurons from postnatal day 1-old wild-type or *Kcnma1*$^{-/-}$ mice (C57BL/6J/129 strain) [36] were cultured in Neurobasal medium with 2% B27 supplement, 0.5 mm glutamine, and 100 U/ml penicillin/streptomycin (Invitrogen, San Diego, CA). Cells were grown at 37°C in a humidified atmosphere containing 5% CO_2 and 95% air. The data in **Fig. 1d**,**2b,2c** and **3b** were done in intact neurons or isolated nuclei of primary cultured hippocampal neurons from postnatal day 1 Sprague-Dawley rat. All experiments were performed on cells cultured for 14 d. DNA transfection was done on DIV 8 by using Lipofectamine 2000 (Invitrogen, San Diego, CA) as described[50]. BK-GFP plasmid was gift from Dr. Xiangdong Tang[51,52]. PV-NLS plasmid was gift from Dr. Michael Nathanson[32]. Kinase-inactive form of CaMKIV (dn CaMKIV, CaMKIVK75E) and CaMBP4 plasmids were gifts from Dr. Hilmar Bading[12]. For shRNA, three different sequences were obtained from Shanghai GeneChem (shBK 1, shBK 2 and shBK 3), cloned and tested for silencing efficiency. shBK (1) and (2) (GTGATGCCAAAGAAGTTAA and GCACTTACGTACTGGGAATGT) was selected. The targeting sequences for all RyRs or RyR2 are ACATGGAGACCAAGTGCTT and GGAAAGAAGTCGATGGCAT, respectively[25]. As control, a scramble version of this sequence was used. For the studies on dendrite morphology, neurons were analyzed 4–5 days after transfection. In lentivirus-delivery shRNA, virus was constructed and packed by Shanghai GeneChem Co.,Ltd, and infection was performed following the manual. 10^7/ml of the virus was used to transfect the cultured hippocampal neurons. The shRNA target sequences of nBK channel-regulated gene are listed below:

Atf3 (1) 5’-TCCTAGCCTGTCAACATAATA-3’,

(2) 5’-TATTATGTTGACAGGCTAGGA-3’.

Npas4 (1) 5’-TCTGTGACTTAACGTCTTCAA-3’,

(2) 5’-GGGCGACAGTATCTACGATAT -3’.

Btg2 (1) 5’- GGACGCACTGACCGATCATTA-3’,

Author Manuscript Author Manuscript Author Manuscript Author Manuscript

(2) 5’-GCTATCGCTGTATCCGTATCA-3’.

c-fos (1) 5’- GCAGATCTGTCCGTCTCTAGT-3’,

(2) 5’-GCTGAAGGCAGAACCCTTTGA-3’.

Bcl6 (1) 5’-GCACGCTAGTGATGTTCTTCT-3’,

(2) 5’-GGACATCTTGACGGACGTTGT-3’.

Ifi202b(1) 5’- GCTACAGAGAGCCAATATTAC-3’,

(2) 5’-GCTGCTCCTAACCAAATTATT-3’.

Western blot

Western blot were performed as described[50]. Briefly, protein concentration was measured by BCA Protein Assay Kit (Thermo). Samples were combined with 2 × SDS loading buffer, boiled for 10 min, and loaded onto 10% or 4–20% gradient polyacrylamide-SDS gel. Proteins were then transferred to a PVDF membrane (Millipore, Billerica, MA) for 2 h at 350 mA, and membranes were incubated in Odyssey Blocking Buffer (LI-COR) for 2 h at room temperature. After incubation with primary antibodies for overnight at 4°C, the blots were washed three times in TBS containing 0.1% Tween 20 for 15 min and then incubated with peroxidase- or IRDye-conjugated secondary antibody for 1 h in TBS, 0.1% Tween 20 at room temperature. Immunoreactivity was detected by chemiluminescence with ECL reagent or LiCor imaging system.

Extraction of plasma membrane protein

For surface biotinylation, neurons were cooled on ice, washed twice with ice-cold PBS containing 1mM $CaCl_2$ and 0.5 mM $MgCl_2$, and then incubated with PBS containing 1mM $CaCl_2$, 0.5 mM $MgCl_2$, and 1 mg/ml Sulfo-NHS-SS-Biotin (Pierce) for 30 min at 4°C. Unreacted biotin was quenched by washing cells three times with ice-cold 100mM Glycine (pH7.4). Cultures were harvested in RIPA buffer. Homogenates were centrifuged at 132,000 rpm for 20 min at 4°C. The resulting supernatant volume was measured and 15% of it separated as the total protein. The remaining 85% of the homogenate was rotated overnight at 4°C with Streptavidin beads (Pierce). Precipitates were washed with RIPA buffer and analyzed by immunoblotting with each antibody.

Nuclei isolation

Cultured neurons were collected and resuspended in Buffer A (2.0 mM $MgCl_2$, 125 mM KCl, 10 mM HEPES (pH 7.5), protease inhibitors). After swelling on ice for 10 min, the cell membrane and cytoskeleton were disrupted by 15 brief homogenization. The solution were filtered with 3 layers of gauze, and then centrifuged with 1000g for 10min. The precipitate were resuspended in Buffer N (0.25 M sucrose in buffer A), and covered on the top of Buffer B (1.1 M sucrose in buffer A) in a centrifuge tube and centrifuged with 1000g for 10 min, at 4°C. We only performed experiments in intact and clean nuclei (free of ER contamination). All the data of isolated nuclei were from at least 3 independent cultures

Author Manuscript Author Manuscript Author Manuscript Author Manuscript

from at least 3 litters. The isolated nuclei were treated with Triton X100 buffer (1% Triton X-100, 100 mM NaCl, 300 mM sucrose, 3 mM $MgCl_2$, 0.5 mM $CaCl_2$,1 mM DTT) for 7 min, and centrifuged with 650 g for 5 min. The resultant precipitate was saved as the denuded nuclei fraction and the supernatant as the nuclear envelope fraction for further analyses. Alternatively, nuclei isolation followed the previous report[31]. Nuclei were prepared by lysing hippocampal neurons at room temperature in PBS (pH 7.2) containing 0.5% (v/v) NP-40, 7.5 mM K^+ 2EGTA, 2.5 mM Ca^{2+}EGTA and 2.5 (free Ca^{2+} concentration is 60 nM). The free Ca^{2+} concentration was increased to 1 μM by adding 6.2 volumes of 10 mM Ca^{2+}EGTA. After 60 to 90 s, 1.8 volumes of 4× sample buffer was added, nuclei were scraped off the dish, boiled for 7 min, and subjected to SDS-PAGE and immunoblot analyses.

Nuclear protein extraction

Nuclear protein was extracted using the PIERCE Nuclear Protein Extraction Kit (Thermo), following the manual. Briefly, cells were collected by centrifugation, 500g for 3 min at 4°C. Resuspend cells in 200μl precooled CER I by 15 sec of intense vortex, and incubate on ice for 10 min. Add 11μl precooled CER II to the solution, and after 5 sec of intense vortex, incubate it on ice for 1 min. After 5 sec of intense vortex, centrifuge the solution at 16000g for 5 min, at 4°C, discard the supernatant. Add 100μl NER to the precipitate and vibrate it intensively for 15 sec, and incubate it on ice for 10 min. Repeat this step 4 times, and then centrifuge the solution at 16000g for 10 min, at 4°C. The supernatant was purified nuclear protein.

Patch-clamp experiments

For whole-cell recordings, electrodes were with a final resistance of 5–10 MΩ when filled with pipette solution (in mM): 120.0 potassium gluconate, 15.0 HEPES, 2.2 CaCl2, 1.0 MgCl2, 4.0 EGTA, and 4.0 HEDTA, pH7.35, 305mOsm. Currents were recorded using an Axopatch 200B (Axon Instruments, Foster City, CA) amplifier at a sampling rate of 1–5 kHz and leak-subtracted on line. Series resistance never exceeded 25 MΩ and was compensated. Data were acquired and analyzed with pClamp9 (Axon Instruments). Single-channel currents were recorded from nuclei positively labeled with ethidium homodimer-1 by using standard patch-clamp recording procedures[24]. Currents were recorded in symmetrical 135 mM K using a patch-clamp amplifier (Axopatch 200; Axon Instruments) at a sampling rate of 5 kHz and filtered at 1 kHz filter. Experiments were performed at RT. High resistance seals were formed (5–7 GΩ), indicating minimal contamination by the endoplasmic reticulum (ER) membrane[24]. Under these circumstances, it has been proposed that nuclear pores would be occluded or nonconducting because of experimental conditions or lack of cytosolic factors[6,39,53]. PCLAMP software was used to measure the current magnitude and duration.

Ca^{2+} imaging

Intact neurons were loading with Fluo-4/AM or X-Rhod-1 AM (Life Technology) in transfected neurons, in HEPPS buffer for 30 min, and washed 3 times before imaging. Single isolated nuclei were loaded as reported[24]. The membrane impermeant Ca^{2+} probe Fluo-4/dextran (30 μg/ml; 30 min at 4°C; Life Technologies) loaded the nucleoplasm while

Author Manuscript Author Manuscript Author Manuscript Author Manuscript

the membrane permeant Ca^{2+} probe Fluo-4/AM (20 μM; 60 min at 4°C) loaded the nuclear envelope. After loading, the nuclei were washed twice with the intracellular medium (125 mM KCl/2 mM K_2HPO_4/40 mM Hepes/0.1 mM $MgCl_2$, pH 7.2/100 nM Ca^{2+}, with 10.2 mM EGTA and 1.65 mM $CaCl_2$) and then were equilibrated in the same medium supplemented with 1 μM of ATP and 300 nM Ca^{2+} for a few minutes to load nuclei with Ca^{2+}. After that, they were washed twice again with the intracellular buffer (without ATP and Ca^{2+}). Experiments were done at RT. No probe leakage was detected during the experiment. Ca^{2+} imaging in single isolated nuclei was performed by using an Olympus FV1000 Confocal microscope. Images were collected at 1 s intervals, and fluorescence was measured by using the Olympus FV1000 software package. The difference (ΔF) between the mean fluorescence measured in a given region of interest (ROI) and the corresponding control value for each ROI (F_0) was expressed as fraction of the control ($\Delta F/F_0$) and was plotted as a function of time.

Nuclear Transmembrane Potential ($\Delta\Psi_n$) Measurements

Isolated nuclei were equilibrated in intracellular medium with $DiOC_6(3)$ (200 nM, RT, Life Technologies), which is a fluorescent cationic lipophyllic dye whose incorporation into lumen is proportional to $\Delta\Psi$[24]. After 10 min, the nuclear envelope became stained. The nuclear were washed for 3 times before imaging with Olympus FV1000 Confocal microscope. Images were collected at 1 s intervals, and fluorescence was measured by using the Olympus FV1000 software package. The difference (ΔF) between the mean fluorescence measured in a given region of interest (ROI) and the corresponding control value for each ROI (F_0) was expressed as fraction of the control ($\Delta F/F_0$) and was plotted as a function of time.

Immunocytochemistry

Cells were washed with PBS and fixed for 20 min with 4% paraformaldehyde at room temperature. To permeabilize cells, cells were treated with 0.3% Triton X-100 in PBS solutions. Nonspecific binding was blocked for 1 h at room temperature using 5% bovine serum. Primary antibodies were then added and incubated overnight at 4 °C. Cells were then washed and incubated for 1 h with the fluorescent-labeled secondary antibodies at room temperature, and washed for three times to remove the unbound antibodies.

Phospho-CREB Immunofluorescence

CREB phosphorylation was induced in isolated nuclei by increasing Ca^{2+} in an EGTA-buffered intracellular medium from 60 nM to 200 nM Ca^{2+} or by addition of paxilline for 3 min. Nuclei were fixed with 4% paraformaldehyde (wt/vol) and permeabilized with 0.1% Triton X-100 for 10 min. Nuclei were preincubated with blocking buffer; then anti-phospho-CREB antibodies were applied for 16 h at 4°C. Phospho-CREB was visualized with TRITC-conjugated secondary antibodies (1 h, RT). High Ca^{2+} gave the maximum response.

Morphometric Analyses

For three-dimensional Sholl analysis, total dendritic length and spine morphology were calculated by using Image-J freeware software. Briefly, a z-stack acquisition was imported,

Author Manuscript Author Manuscript Author Manuscript Author Manuscript

calibrated in Image-J, and manually traced. Total dendritic length was then computed. For Sholl analysis, the shell interval was set at 10 μm. All analyses were performed blind.

RNA Extraction and cDNA Synthesis

Total RNA was isolated from hippocampal primary neuron cultures with RNeasy Mini Kit (TAKARA) including an optional DNase I treatment at room temperature for 15 min according to manufacturer's instructions (TAKARA). 1.2 μg of extracted RNA was reverse transcribed into first strand cDNA using High Capacity cDNA Reverse Transcription kit (Applied Biosystems, Foster City, CA).

Real Time Quantitative PCR

Quantitative reverse transcriptase PCR (qRT-PCR) was done on a Statagene Mx3000P thermal cycler using Universal qRT-PCR master mix for the indicated genes (TAKARA). The primers were designed and synthesized as follow:

c-Fos sense 5'- GCGGGAGTGGTGAAGACCAT-3',

antisense 5'- GCTTGGAGCGTATCTGTCAGCTC-3'.

Npas4 sense 5'- ACATCATGAGTCTTGCCTGCATC-3',

antisense 5'- TCCAGGTAGTGCTGCCACTATGTC-3'.

Atf3 sense 5'- ATGATGCTTCAACACCCAGGC-3'

antisense 5'- TTAGCTCTGCAATGTTCCTTC-3'

Btg2 sense 5'- GAGCGAGCAGAGACTCAAGGTT-3',

antisense 5'- CGATAGCCAGAACCTTTGGATGG-3'.

Bcl6 sense 5'- CAGAGATGTGCCTCCATACTGC-3',

antisense 5'- CTCCTCAGAGAAACGGCAGTCA-3'.

Ifi202b AAGAAAGGCTGGTTGATGGAGAG-3',

antisense 5'- GGTCAGTTGTCCAGATACCACC-3'.

GADD45β sense 5'- GGAGACATTGGGCACAACCGAA-3',

antisense 5'- CTGCTCTCTTCACAGTAACTGGC-3'.

GADD45γ sense 5'- TCTACGAGTCCGCCAAAGTCCT-3',

antisense 5'- CTCACAGCAGAACGCCTGAATC-3'.

GAPDH sense 5'-GGCACAGTCAAGGCTGAGAATG-3',

antisense 5'-ATGGTGGTGAAGACGCCAGTA-3'.

Author Manuscript Author Manuscript Author Manuscript Author Manuscript

Expression of target genes was normalized against the expression of GAPDH as endogenous control gene. Data were derived from cells from 3 independent cultures from at least 3 litters.

Statistical Analysis

SPSS 13.0 was used for statistical analysis. The data were collected and processed randomly. No statistical methods were used to predetermine sample size, but our sample sizes are similar to those reported in previous publications.[50,54–57] Statistical significances were determined by comparing means of different groups using unpaired t-test or one-way ANOVA followed by Fisher's least significant difference (LSD) test. Two-sided test was used in the analysis. Data met the assumptions of the statistical tests used, and equal variances were formally tested. The criterion for excluding data points were established prior to data collection. An outlier was defined as a value outside the mean ± 3 s.d.. All the immunocytochemistry, immunoelectron microscopy imaging, sholl analysis, qRT-PCR, calcium imaging and electrophysiology experiments were carried out blind. The western blot was not blind when loading the samples, but data collection and analyses were performed blind. For the box and whisker plot, the bottom and top of the box are the first and third quartiles, and the band inside the box is the median. The whisker represents the minimum and maximum of all of the data. The data were expressed as mean ± s.e.m. if not otherwise specified.

Supplementary Material

Refer to Web version on PubMed Central for supplementary material.

Acknowledgment

We thank Dr. Xiangdong Tang (Nankai University) for BK-GFP plasmid, Dr. Michael Nathanson (Yale University) for PV-NLS plasmid, Dr. Hilmar Bading (University of Heidelberg) for CaMKIVK75E and CaMBP4 plasmids, Dr. Feng-Xia Liang and Microscopy Core of New York University Medical Center for immunoelectron microscopy analysis. This work was supported by the National Natural Science Foundation of China (Grants 81030022; 81329003; U1201225 to TM.G., 30900581 to B.L., 81001129 to L.H.), the Program for Changjiang Scholars and Innovative Research Team (Grant IRT1142), Guangdong Natural Science Foundation (Grant 9351051501000003; CXZD1018 to TM.G., 10451051501004726 to L.H.), Guangzhou Science and Technology Project (Grant 7411802013939), Medical Scientific Research Foundation of Guangdong Province (B2010170 to L.H.), the National Heart, Lung, and Blood Institute (Grant R01-HL102758 to A.L.M.).

References

1. Wheeler DG, et al. Ca(V)1 and Ca(V)2 channels engage distinct modes of Ca(2+) signaling to control CREB-dependent gene expression. Cell. 2012; 149:1112–1124. [PubMed: 22632974]
2. Jiang D, Zhao L, Clapham DE. Genome-wide RNAi screen identifies Letm1 as a mitochondrial Ca2+/H+ antiporter. Science. 2009; 326:144–147. [PubMed: 19797662]
3. Calcraft PJ, et al. NAADP mobilizes calcium from acidic organelles through two-pore channels. Nature. 2009; 459:596–600. [PubMed: 19387438]
4. Dong XP, et al. The type IV mucolipidosis-associated protein TRPML1 is an endolysosomal iron release channel. Nature. 2008; 455:992–996. [PubMed: 18794901]
5. Wegierski T, et al. TRPP2 channels regulate apoptosis through the Ca2+ concentration in the endoplasmic reticulum. EMBO J. 2009; 28:490–499. [PubMed: 19153608]
6. Bootman MD, Fearnley C, Smyrnias I, MacDonald F, Roderick HL. An update on nuclear calcium signalling. J.Cell Sci. 2009; 122:2337–2350. [PubMed: 19571113]

Author Manuscript Author Manuscript Author Manuscript Author Manuscript

7. Carafoli E, Nicotera P, Santella L. Calcium signalling in the cell nucleus. Cell Calcium. 1997; 22:313–319. [PubMed: 9448938]
8. Gerasimenko OV, Gerasimenko JV, Tepikin AV, Petersen OH. ATP-dependent accumulation and inositol trisphosphate- or cyclic ADP-ribose-mediated release of Ca2+ from the nuclear envelope. Cell. 1995; 80:439–444. [PubMed: 7859285]
9. Leite MF, et al. Nuclear and cytosolic calcium are regulated independently. Proc Natl Acad Sci U S A. 2003; 100:2975–2980. [PubMed: 12606721]
10. Stehno-Bittel L, Luckhoff A, Clapham DE. Calcium release from the nucleus by InsP3 receptor channels. Neuron. 1995; 14:163–167. [PubMed: 7530018]
11. Bading H. Nuclear calcium signalling in the regulation of brain function. Nat.Rev.Neurosci. 2013; 14:593–608. [PubMed: 23942469]
12. Zhang SJ, et al. Nuclear calcium signaling controls expression of a large gene pool: identification of a gene program for acquired neuroprotection induced by synaptic activity. PLoS.Genet. 2009; 5:e1000604. [PubMed: 19680447]
13. Mauceri D, Freitag HE, Oliveira AM, Bengtson CP, Bading H. Nuclear calcium-VEGFD signaling controls maintenance of dendrite arborization necessary for memory formation. Neuron. 2011; 71:117–130. [PubMed: 21745642]
14. Limback-Stokin K, Korzus E, Nagaoka-Yasuda R, Mayford M. Nuclear calcium/calmodulin regulates memory consolidation. J.Neurosci. 2004; 24:10858–10867. [PubMed: 15574736]
15. Papadia S, Stevenson P, Hardingham NR, Bading H, Hardingham GE. Nuclear Ca2+ and the cAMP response element-binding protein family mediate a late phase of activity-dependent neuroprotection. J.Neurosci. 2005; 25:4279–4287. [PubMed: 15858054]
16. Misonou H, et al. Immunolocalization of the Ca2+-activated K+ channel Slo1 in axons and nerve terminals of mammalian brain and cultured neurons. J Comp Neurol. 2006; 496:289–302. [PubMed: 16566008]
17. Douglas RM, et al. The calcium-sensitive large-conductance potassium channel (BK/MAXI K) is present in the inner mitochondrial membrane of rat brain. Neuroscience. 2006; 139:1249–1261. [PubMed: 16567053]
18. Singh H, et al. MitoBK(Ca) is encoded by the Kcnma1 gene, and a splicing sequence defines its mitochondrial location. Proc Natl Acad Sci U S A. 2013; 110:10836–10841. [PubMed: 23754429]
19. Gong LW, Gao TM, Huang H, Zhuang ZY, Tong Z. Transient forebrain ischemia induces persistent hyperactivity of large conductance Ca2+-activated potassium channels via oxidation modulation in rat hippocampal CA1 pyramidal neurons. Eur.J.Neurosci. 2002; 15:779–783. [PubMed: 11886457]
20. Hu H, et al. Presynaptic Ca2+-activated K+ channels in glutamatergic hippocampal terminals and their role in spike repolarization and regulation of transmitter release. J Neurosci. 2001; 21:9585–9597. [PubMed: 11739569]
21. Lee US, Cui J. BK channel activation: structural and functional insights. Trends Neurosci. 2010; 33:415–423. [PubMed: 20663573]
22. Salkoff L, Butler A, Ferreira G, Santi C, Wei A. High-conductance potassium channels of the SLO family. Nat.Rev.Neurosci. 2006; 7:921–931. [PubMed: 17115074]
23. Fricker M, Hollinshead M, White N, Vaux D. Interphase nuclei of many mammalian cell types contain deep, dynamic, tubular membrane-bound invaginations of the nuclear envelope. J Cell Biol. 1997; 136:531–544. [PubMed: 9024685]
24. Quesada I, et al. Nuclear KATP channels trigger nuclear Ca(2+) transients that modulate nuclear function. Proc Natl Acad Sci U S A. 2002; 99:9544–9549. [PubMed: 12089327]
25. Wu B, Yamaguchi H, Lai FA, Shen J. Presenilins regulate calcium homeostasis and presynaptic function via ryanodine receptors in hippocampal neurons. Proc.Natl.Acad.Sci.U.S.A. 2013; 110:15091–15096. [PubMed: 23918386]
26. Deisseroth K, Mermelstein PG, Xia H, Tsien RW. Signaling from synapse to nucleus: the logic behind the mechanisms. Curr.Opin.Neurobiol. 2003; 13:354–365. [PubMed: 12850221]
27. Han MH, et al. Role of cAMP response element-binding protein in the rat locus ceruleus: regulation of neuronal activity and opiate withdrawal behaviors. J.Neurosci. 2006; 26:4624–4629. [PubMed: 16641242]

Author Manuscript Author Manuscript Author Manuscript Author Manuscript

28. Sheng M, Thompson MA, Greenberg ME. CREB: a Ca(2+)-regulated transcription factor phosphorylated by calmodulin-dependent kinases. Science. 1991; 252:1427–1430. [PubMed: 1646483]
29. Bito H, Deisseroth K, Tsien RW. CREB phosphorylation and dephosphorylation: a Ca(2+)-and stimulus duration-dependent switch for hippocampal gene expression. Cell. 1996; 87:1203–1214. [PubMed: 8980227]
30. Xing J, Ginty DD, Greenberg ME. Coupling of the RAS-MAPK pathway to gene activation by RSK2, a growth factor-regulated CREB kinase. Science. 1996; 273:959–963. [PubMed: 8688081]
31. Hardingham GE, Arnold FJ, Bading H. Nuclear calcium signaling controls CREB-mediated gene expression triggered by synaptic activity. Nat Neurosci. 2001; 4:261–267. [PubMed: 11224542]
32. Rodrigues MA, et al. Nucleoplasmic calcium is required for cell proliferation. J.Biol.Chem. 2007; 282:17061–17068. [PubMed: 17420246]
33. Lin Y, et al. Activity-dependent regulation of inhibitory synapse development by Npas4. Nature. 2008; 455:1198–1204. [PubMed: 18815592]
34. Ramamoorthi K, et al. Npas4 regulates a transcriptional program in CA3 required for contextual memory formation. Science. 2011; 334:1669–1675. [PubMed: 22194569]
35. Meredith AL, Thorneloe KS, Werner ME, Nelson MT, Aldrich RW. Overactive bladder and incontinence in the absence of the BK large conductance Ca2+-activated K+ channel. J.Biol.Chem. 2004; 279:36746–36752. [PubMed: 15184377]
36. Meredith AL, et al. BK calcium-activated potassium channels regulate circadian behavioral rhythms and pacemaker output. Nat.Neurosci. 2006; 9:1041–1049. [PubMed: 16845385]
37. Sausbier M, et al. Cerebellar ataxia and Purkinje cell dysfunction caused by Ca2+-activated K+ channel deficiency. Proc.Natl.Acad.Sci.U.S.A. 2004; 101:9474–9478. [PubMed: 15194823]
38. Xu W, et al. Cytoprotective role of Ca2+- activated K+ channels in the cardiac inner mitochondrial membrane. Science. 2002; 298:1029–1033. [PubMed: 12411707]
39. Mazzanti M, Bustamante JO, Oberleithner H. Electrical dimension of the nuclear envelope. Physiol Rev. 2001; 81:1–19. [PubMed: 11152752]
40. Dick DA. The distribution of sodium, potassium and chloride in the nucleus and cytoplasm of Bufo bufo oocytes measured by electron microprobe analysis. J Physiol. 1978; 284:37–53. [PubMed: 104029]
41. Garner MH. Na,K-ATPase in the nuclear envelope regulates Na+: K+ gradients in hepatocyte nuclei. J Membr Biol. 2002; 187:97–115. [PubMed: 12029368]
42. Gifford JD, Galla JH, Luke RG, Rick R. Ion concentrations in the rat CCD: differences between cell types and effect of alkalosis. The American journal of physiology. 1990; 259:F778–782. [PubMed: 2240232]
43. Rick R. pHi determines rate of sodium transport in frog skin: results of a new method to determine pHi. The American journal of physiology. 1994; 266:F367–374. [PubMed: 8160784]
44. Endo M. Calcium-induced calcium release in skeletal muscle. Physiol Rev. 2009; 89:1153–1176. [PubMed: 19789379]
45. Chen SR, Li X, Ebisawa K, Zhang L. Functional characterization of the recombinant type 3 Ca2+ release channel (ryanodine receptor) expressed in HEK293 cells. J Biol Chem. 1997; 272:24234–24246. [PubMed: 9305876]
46. Zahradnikova A, Meszaros LG. Voltage change-induced gating transitions of the rabbit skeletal muscle Ca2+ release channel. J Physiol. 1998; 509(Pt 1):29–38. [PubMed: 9547378]
47. van WI, du LS. Bidirectional control of BK channel open probability by CAMKII and PKC in medial vestibular nucleus neurons. J.Neurophysiol. 2011; 105:1651–1659. [PubMed: 21307321]
48. Loane DJ, Hicks GA, Perrino BA, Marrion NV. Inhibition of BK channel activity by association with calcineurin in rat brain. Eur.J.Neurosci. 2006; 24:433–441. [PubMed: 16903851]
49. Shamloo M, et al. Npas4, a novel helix-loop-helix PAS domain protein, is regulated in response to cerebral ischemia. Eur.J.Neurosci. 2006; 24:2705–2720. [PubMed: 17156197]
50. Huang L, Li B, Li W, Guo H, Zou F. ATP-sensitive potassium channels control glioma cells proliferation by regulating ERK activity. Carcinogenesis. 2009; 30:737–744. [PubMed: 19176641]

Author Manuscript Author Manuscript Author Manuscript Author Manuscript

51. Avdonin V, Tang XD, Hoshi T. Stimulatory action of internal protons on Slo1 BK channels. Biophys J. 2003; 84:2969–2980. [PubMed: 12719228]

52. Tang XD, et al. Haem can bind to and inhibit mammalian calcium-dependent Slo1 BK channels. Nature. 2003; 425:531–535. [PubMed: 14523450]

53. Taylor CW, et al. IP3 receptors: some lessons from DT40 cells. Immunol.Rev. 2009; 231:23–44. [PubMed: 19754888]

54. Cao X, et al. Astrocyte-derived ATP modulates depressive-like behaviors. Nature medicine. 2013; 19:773–777.

55. Woo RS, et al. Neuregulin-1 enhances depolarization-induced GABA release. Neuron. 2007; 54:599–610. [PubMed: 17521572]

56. Chen YJ, et al. ErbB4 in parvalbumin-positive interneurons is critical for neuregulin 1 regulation of long-term potentiation. Proc Natl Acad Sci U S A. 2010; 107:21818–21823. [PubMed: 21106764]

57. Li XM, et al. Contribution of downregulation of L-type calcium currents to delayed neuronal death in rat hippocampus after global cerebral ischemia and reperfusion. J Neurosci. 2007; 27:5249–5259. [PubMed: 17494711]

Author Manuscript Author Manuscript Author Manuscript Author Manuscript

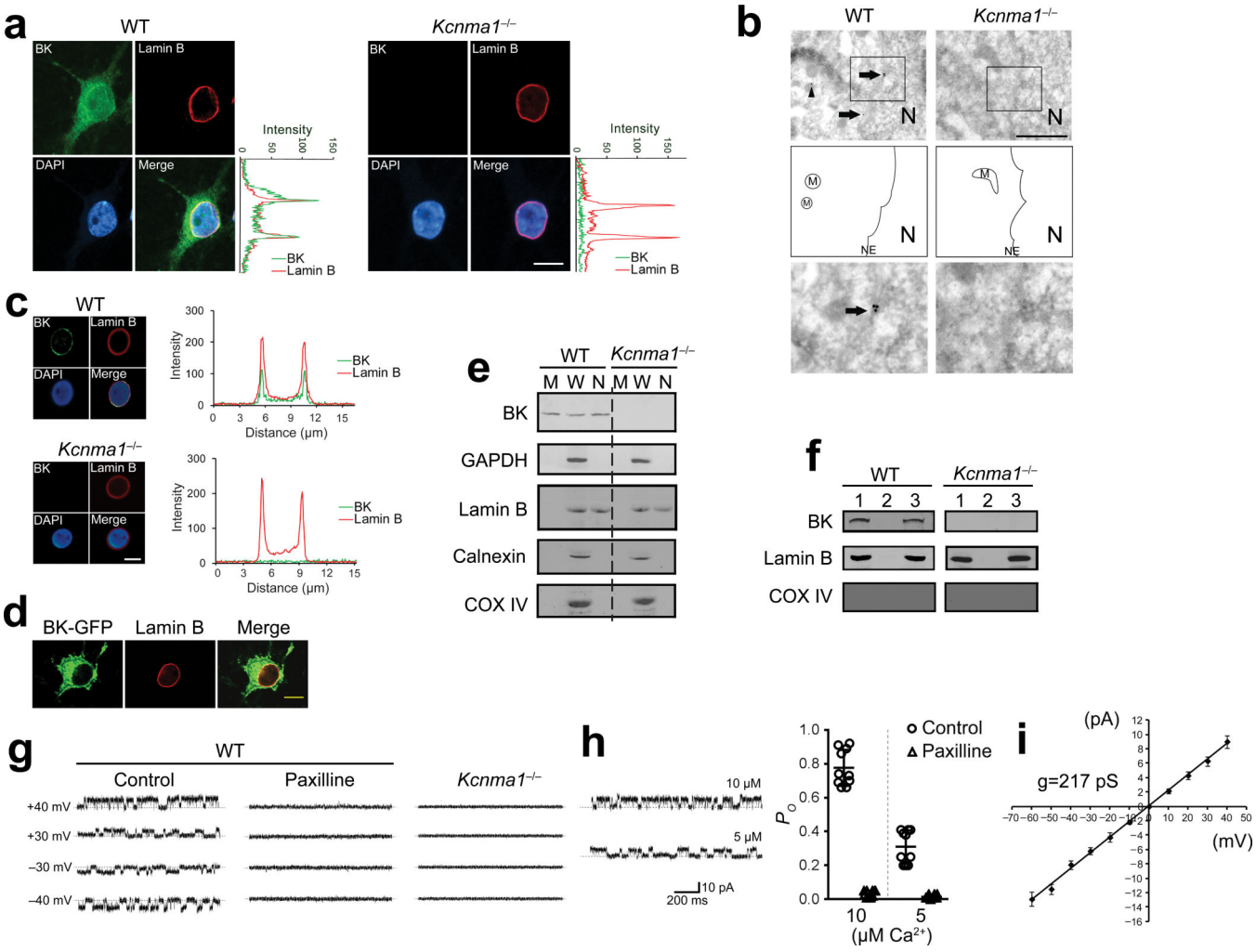

Figure 1. BK channels expression on the NE of hippocampal neurons

(a) The confocal immunofluorescence of BK channel and lamin B in cultured hippocampal neurons. Analysis of intensity profiles of the vertical line across the center of the nucleus was shown on the right. Over 85% of the neurons (>100 neurons) have the positive BK channel staining in NE. (**b**) Immunoelectron microscopy images of BK channel localization in cultured hippocampal neurons (Top). Gold particles signaling BK channels were localized on NE (arrows) and mitochondria (M) (arrowhead) in wild-type mice. Forty-six immunoelectron microscopy images were taken totally. NE–localized gold particles were observed in all the images from the wild-type mice, and there is no signal in *Kcnma1*$^{-/-}$ mice. Scale bar represents 1 μm. Middle, schematic diagram of the top images. Bottom, an enlargement of a square region indicated in the top images. (**c**) Left, immunofluorescence of BK channels and lamin B in isolated nuclei. Right, analysis of intensity profiles of the horizontal line across the center of the isolated nuclei. (**d**) Immunofluorescence of BK-GFP and lamin B. (**e**) Western blot results of the subcellular localization of the BK channel in the membrane fraction (M), the whole cell lysate (W), and the nuclear fraction (N). (**f**) Western blot results of the BK channel expression in intact isolated nuclei (1), denuded nuclei (2) and NE (3). (**g**) Single channel activities of the BK channel in isolated nuclei with 10 μM Ca^{2+} at

Author Manuscript Author Manuscript Author Manuscript Author Manuscript

different voltage in control group (left), with paxilline treatment (10 μM, middle), and in the nuclei from *Kcnma1*$^{-/-}$ mice (right) (n = 6). (**h**) Left, single channel activities recorded in the solutions with 10 μM or 5 μM Ca^{2+} at 40 mV. Right, BK channel open probability (P_O) recorded in the solutions with 10 μM (n = 10 for each group, unpaired t-test, $P = 2.30 \times 10^{-14}$, $t_{18} = 21.71$ between control and paxilline) or 5 μM Ca^{2+} (n = 10 for each group, unpaired t-test, $P = 1.80 \times 10^{-8}$, $t_{18} = 9.55$, between control and paxilline) at 40 mV (error bars are mean ± s.d.). (**i**) I-V curve of the channel activity. For single channel recording, BK channel activity was recorded from 15 of the 20 successful patching of the nuclei from wild-type mice. All the data are from 3 independent cultures from at least 3 litters. All the experiments of **a**–**f** were successfully repeated for at least 3 times. WT, wild-type. Scale bars in **a**,**c**,**d** represent 10 μm. The full-length blots for **e** and **f** are presented in **Supplementary Figure 7**.

Author Manuscript Author Manuscript Author Manuscript Author Manuscript

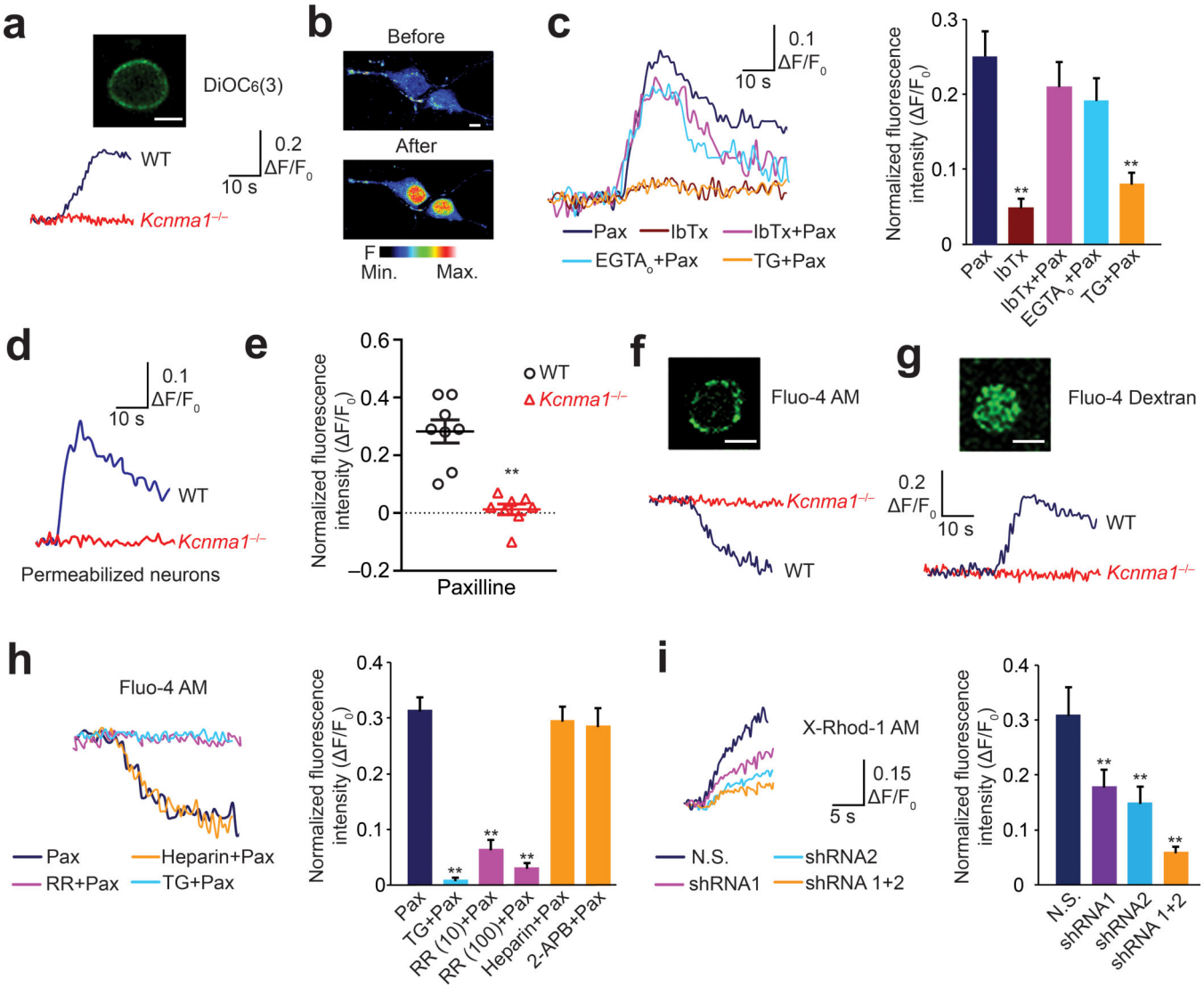

Figure 2. nBK channels regulate the nuclear transmembrane potential and nuclear Ca^{2+} concentration in intact neurons and isolated nuclei

(**a**) Fluorescence intensity changes of $DiOC_6(3)$-loaded isolated nuclei (insert) upon addition of paxilline. (**b**) Confocal nuclear calcium imaging with Fluo-4/AM of the mid-nuclear region in hippocampal neurons. (**c**) The changes of fluorescence intensity in nuclear calcium imaging of intact neurons after indicated treatments (left). Right, summary of the data. One-way ANOVA (n = 15 for each group, $P = 4.70 \times 10^{-7}$, $F_{4,70} = 11.15$) and *post hoc* test. (**d**) Fluorescence intensity changes in the nuclei of digitonin-permeabilized neurons after paxilline treatment. (**e**) Paxilline-induced fluorescence intensity changes in intact neurons from wild-type and *Kcnma1*$^{-/-}$ mice (n = 8 for each group, unpaired t-test, $P = 2.56 \times 10^{-5}$, $t_{14} = 6.14$, points with error bars represent the mean ± s.e.m.). Paxilline-induced changes in Fluo-4/AM (**f**) or Fluo-4/dextran (**g**) fluorescence intensity in the isolated nuclei. (**h**) The changes of fluorescence intensity in isolated nuclei after indicated treatments (left). Right, summary of the data. One-way ANOVA (n = 11, 8, 12, 8, 10, 10, respectively, $P = 2.50 \times 10^{-13}$, $F_{5,53} = 26.55$) and *post hoc* test. (**i**) The changes of fluorescence intensity in isolated

Author Manuscript Author Manuscript Author Manuscript Author Manuscript

nuclei after knockdown of RyRs (left). Right, summary of the data. One-way ANOVA (n = 5, 6, 6, 5, respectively, $P = 0.0016$, $F_{3,18} = 7.72$) and *post hoc* test. Fisher's least significant difference test was used for *post hoc* test in one-way ANOVA. Error bars represent the mean ± s.e.m.. All the data are from 3 independent cultures from at least 3 litters. All the experiments were successfully repeated for at least 3 times. $^{**}P < 0.01$. WT, wild-type; Pax, paxilline; RR, ruthenium red; TG, thapsigargin; shRNA, RyRs-specific shRNAs; N.S., non-silencing shRNAs. Scale bars in **a**,**b**,**f,g** represent 5 μm.

Author Manuscript Author Manuscript Author Manuscript Author Manuscript

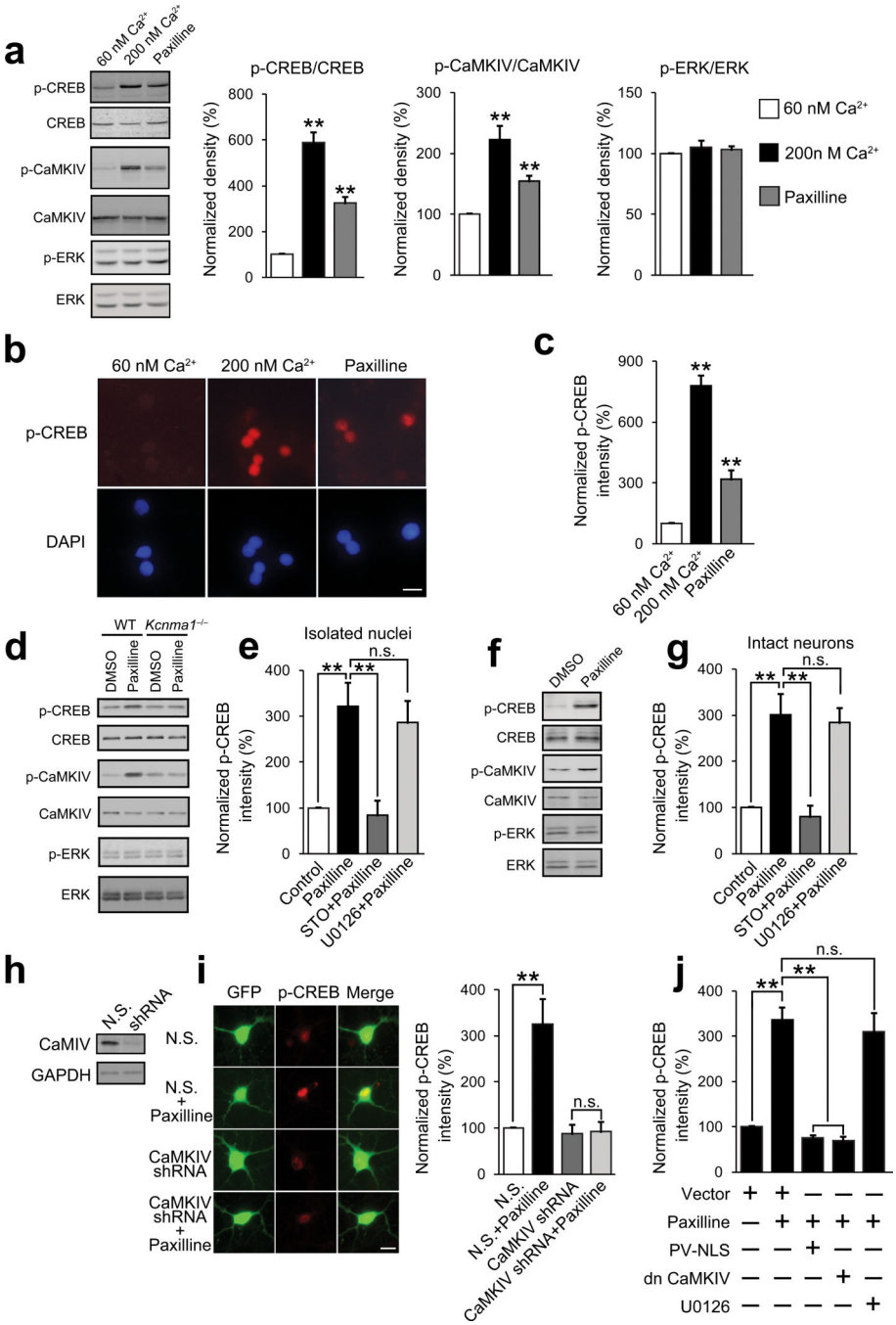

Figure 3. Blockade of nBK channels induces CREB phosphorylation in isolated nuclei and intact neurons

(**a**) Immunoblots of isolated functional nuclei after stimulation as indicated. One-way ANOVA (n = 4 for each group; $P = 1.75 \times 10^{-5}$, $F_{2,9} = 46.81$ for p-CREB; $P = 0.0018$, $F_{2,9} = 13.91$ for p-CaMKIV; $P = 0.87$, $F_{2,9} = 0.14$ for p-ERK) and *post hoc* test. (**b**) Immunofluorescence of CREB phosphorylation. (**c**) Statistic results of **b**. One-way ANOVA (N = 5 for each group, $P = 3.89 \times 10^{-6}$, $F_{2,12} = 41.85$) and *post hoc* test. (**d**,**f**) Immunoblots of isolated functional nuclei (**d**) and intact neurons (**f**) after paxilline treatment. (**e**,**g**)

Author Manuscript Author Manuscript Author Manuscript Author Manuscript

Immunofluorescence intensity of CREB phosphorylation in isolated functional nuclei (**e**) and intact neurons (**g**) after treatments as indicated. One-way ANOVA ($N = 5$ for each group; $P = 0.0093$, $F_{3,16} = 5.40$ for data in **e**; $P = 0.00096$, $F_{3,16} = 9.08$ for data in **g**) and *post hoc* test. (**h**) CaMKIV expression after shRNA transfection. (**i**) Left, paxilline-induced CREB phosphorylation in the neurons transfected with GFP-tagged plasmids encoding CaMKIV-specific shRNAs or non-silencing shRNAs (N.S.), respectively. Right, summary of the data. One-way ANOVA ($N = 5$ for each group, $P = 0.0021$, $F_{3,16} = 7.67$) and *post hoc* test. (**j**) Paxilline-induced CREB phosphorylation after treatments as indicated. One-way ANOVA ($N = 5$ for each group, $P = 5.64 \times 10^{-6}$, $F_{4,20} = 15.76$) and *post hoc* test. Fisher's least significant difference test was used for *post hoc* test in one-way ANOVA. Error bars represent the mean ± s.e.m.. All the data in **a** are from 3 independent cultures from at least 3 litters. All the other data are from 5 coverslips of cells from 3 independent cultures from at least 3 litters. All the experiments were successfully repeated for at least 3 times. $^{**}P < 0.01$; n.s., no significant difference. WT, wild-type; N.S., non-silencing shRNAs. Scale bars in **b**,**h** represent 10 μm. The full-length blots for **a**, **d**, **f** and **h** are presented in **Supplementary Figure 7**.

Author Manuscript Author Manuscript Author Manuscript Author Manuscript

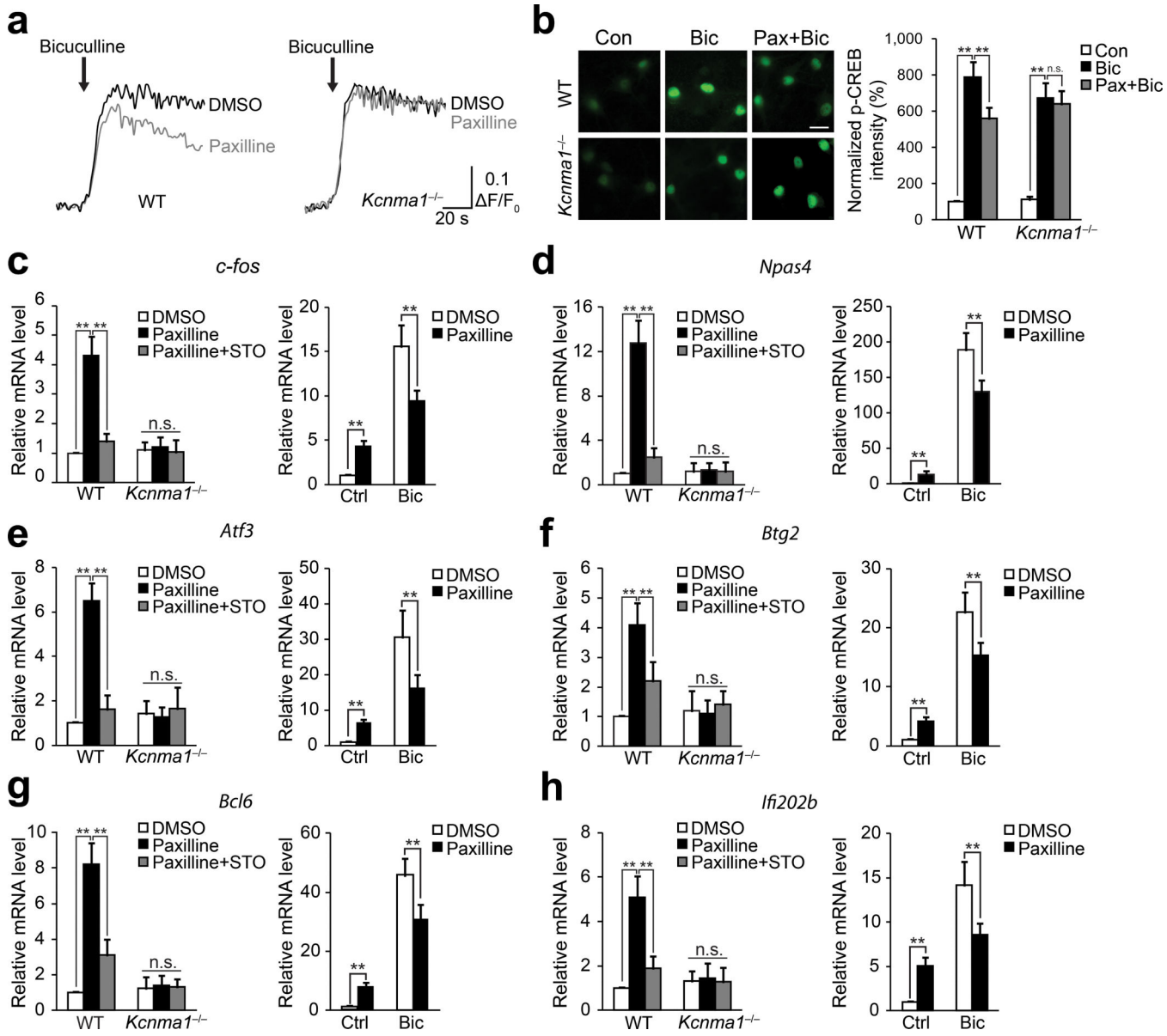

Figure 4. nBK channels regulate synaptic activity-evoked $[Ca^{2+}]_{nu}$ elevation, CREB phosphorylation and gene expression

(**a**) Bicuculline-induced changes of fluorescence intensity in nuclear calcium imaging of intact neurons after DMSO or paxilline pretreatment. (**b**) Left, bicuculline-induced CREB phophorylation in intact neurons with or without paxilline pretreatment. Scale bar represents 20 μm. Right, summary of the data. One-way ANOVA ($N = 5$ for each group; $P = 4.98 \times 10^{-5}$, $F_{2,12} = 25.29$ for wild-type group, $P = 3.15 \times 10^{-5}$, $F_{2,12} = 27.76$ for *Kcnma1*$^{-/-}$ group) and *post hoc* test. (**c**) Left, mRNA level of *c-fos* after treatments as indicated. One-way ANOVA ($P = 0.0015$, $F_{2,6} = 23.34$ for wild-type group; $P = 0.90$, $F_{2,6} = 0.11$ for *Kcnma1*$^{-/-}$ group) and *post hoc* test. Right, bicuculline-induced *c-fos* expression after DMSO or paxilline pretreatment (unpaired *t*-test, $P = 0.0053$, $t_4 = -5.50$ for control group; $P = 0.0093$, $t_4 = 4.70$ for bicuculline group). (**d**) Left, mRNA level of *Npas4* after treatments

Author Manuscript Author Manuscript Author Manuscript Author Manuscript

as indicated. One-way ANOVA (P = 0.00090, $F_{2,6}$ = 28.02 for wild-type group; P = 0.99, $F_{2,6}$ = 0.00999 for *Kcnma1*$^{-/-}$ group) and *post hoc* test. Right, bicuculline-induced *Npas4* expression after DMSO or paxilline pretreatment (unpaired *t*-test, P = 0.0035, t_4 = –6.16 for control group; P = 0.0082, t_4 = 4.87 for bicuculline group). (**e**) Left, mRNA level of *Atf3* after treatments as indicated. One-way ANOVA (P = 0.00048, $F_{2,6}$ = 35.38 for wild-type group; P = 0.90, $F_{2,6}$ = 0.11 for *Kcnma1*$^{-/-}$ group) and *post hoc* test. Right, bicuculline-induced *Atf3* expression after DMSO or paxilline pretreatment (unpaired *t*-test, $P = 4.29 \times 10^{-5}$, t_4 = –19.25 for control group; P = 0.0023, t_4 = 6.88 for bicuculline group). (**f**) Left, mRNA level of *Btg2* after treatments as indicated. One-way ANOVA (P = 0.018, $F_{2,6}$ = 8.36 for wild-type group; P = 0.16, $F_{2,6}$ = 0.16 for *Kcnma1*$^{-/-}$ group) and *post hoc* test. Right, bicuculline-induced *Btg2* expression after DMSO or paxilline pretreatment (unpaired *t*-test, P = 0.0076, t_4 = –4.98 for control group; P = 0.0057, t_4 = 5.40 for bicuculline group). (**g**) Left, mRNA level of *Bcl6* after treatments as indicated. One-way ANOVA (P = 0.0011, $F_{2,6}$ = 25.61 for wild-type group; P = 0.93, $F_{2,6}$ = 0.074 for *Kcnma1*$^{-/-}$ group) and *post hoc* test. Right, bicuculline-induced *Bcl6* expression after DMSO or paxilline pretreatment (unpaired *t*-test, P = 0.0034, t_4 = –6.21 for control group; P = 0.0040, t_4 = 5.96 for bicuculline group). (**h**) Left, mRNA level of *Ifi202b* after treatments as indicated. One-way ANOVA (P = 0.011, $F_{2,6}$ = 10.45 for wild-type group; P = 0.93, $F_{2,6}$ = 0.075 for *Kcnma1*$^{-/-}$ group) and *post hoc* test. Right, bicuculline-induced *Ifi202b* expression after DMSO or paxilline pretreatment (unpaired *t*-test, P = 0.0094, t_4 = –4.69 for control group; P = 0.0030, t_4 = 6.44 for bicuculline group). N = 3 independent cultures from at least 3 litters for each group in **c**–**h**. Fisher's least significant difference test was used for *post hoc* test in one-way ANOVA. Error bars represent the mean ± s.e.m.. $^{**}P < 0.01$; n.s., no significant difference. WT, wild-type.

Author Manuscript Author Manuscript Author Manuscript Author Manuscript

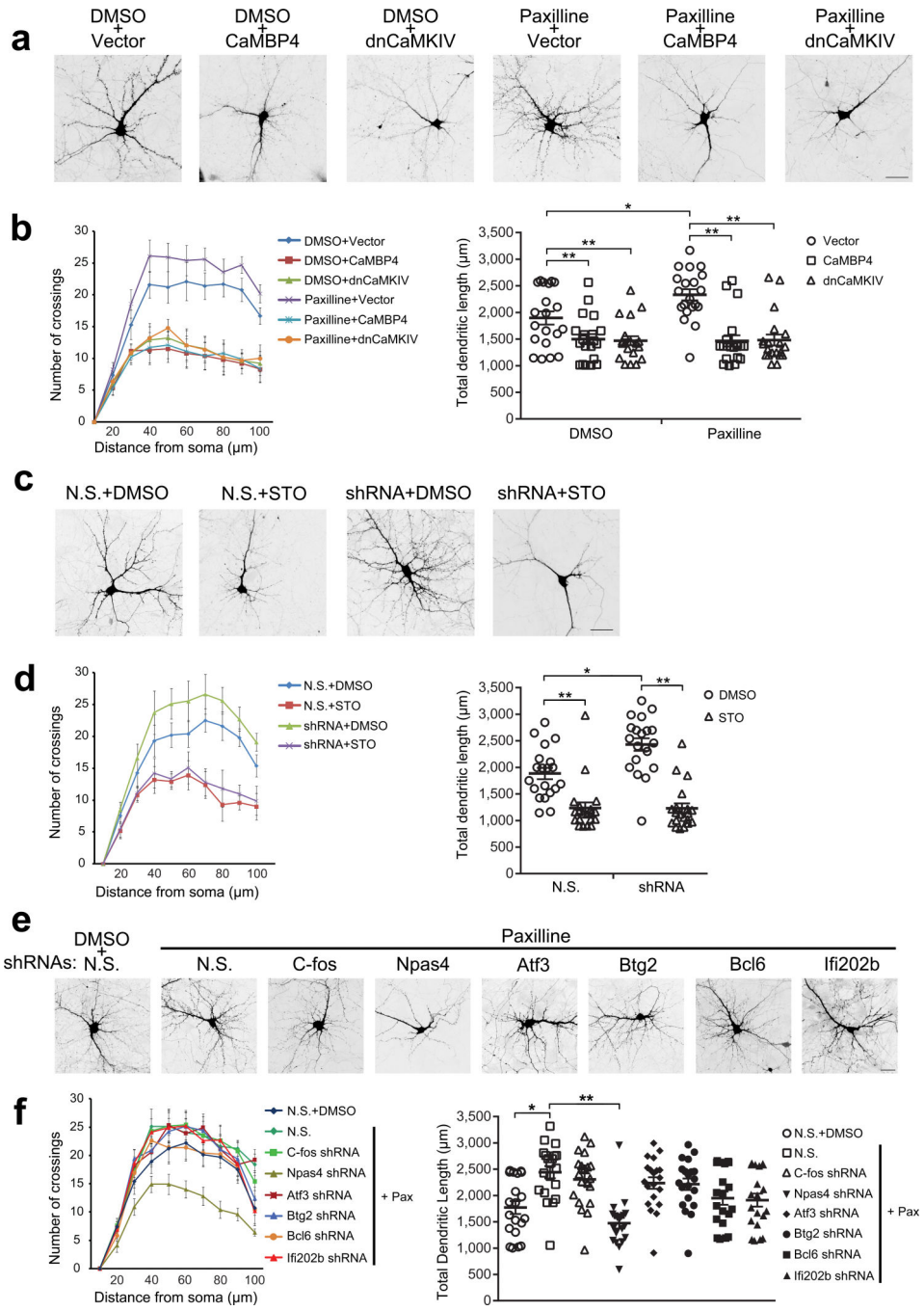

Figure 5. nBK channels regulate dendritic arborization via nuclear Ca^{2+}/CaMKIV signaling

(**a**) Representative micrographs of hippocampal neurons transfected with an expression vector for GFP or cotransfected with expression vectors for GFP and CaMBP4 or for GFP and CaMKIVK75E (dnCaMKIV), with DMSO or paxilline treatment. (**b**) Sholl analysis (left) and quantification of total dendritic length (right) in hippocampal neurons treated as indicated. Right, one-way ANOVA ($P = 0.0070$, $F_{2,57} = 5.42$ for DMSO group; $P = 6.22 \times 10^{-8}$, $F_{2,57} = 22.51$ for paxilline group) and *post hoc* test; unpaired *t*-test ($P = 0.010$, $t_{38} = -2.70$) for comparison between vector groups after DMSO or paxilline treatment. (**c**)

Author Manuscript Author Manuscript Author Manuscript Author Manuscript

Representative micrographs of hippocampal neurons transfected with GFP-tagged plasmids containing BK channel-specific shRNAs or non-silencing shRNAs, with DMSO or STO-609 treatment. (**d**) Sholl analysis (left) and quantification of total dendritic length (right) in hippocampal neurons treated as indicated. Right, unpaired *t*-test ($P = 0.00011$, $t_{38} = 4.32$ for non-silencing shRNAs group; $P = 0.0015$, $t_{38} = -3.42$ for BK channel-specific shRNAs group; $P = 1.17 \times 10^{-9}$, $t_{38} = 7.99$ for comparison between DMSO groups after non-silencing shRNAs or BK channel-specific shRNAs transfection). (**e**) Representative micrographs of hippocampal neurons transfected with GFP-tagged plasmids containing gene-specific shRNAs or non-silencing shRNAs, with DMSO or paxilline treatment. (**f**) Sholl analysis (left) and quantification of total dendritic length (right) in hippocampal neurons treated as indicated. Right, one-way ANOVA ($P = 6.80 \times 10^{-8}$, $F_{7,152} = 7.64$) and *post hoc* test. For the data in **b**,**d**,**f**, $n = 20$ cells from 4 independent cultures from at least 4 litters for each group. Fisher's least significant difference test was used for *post hoc* test in one-way ANOVA. Error bars represent the mean ± s.e.m.. Scale bar = 30 μm. $^{*}P < 0.05$, $^{**}P < 0.01$. N.S., non-silencing shRNAs.